Fate of the organophosphate insecticide, chlorpyrifos, in leaves, soil, and air following application

Supta Das[†], Kimberly J. Hageman[§*], Madeleine Taylor[†],
Sue Michelsen-Heath[‡], Ian Stewart[†]

[†]Department of Chemistry, University of Otago, Dunedin, New Zealand
[§]Department of Chemistry and Biochemistry, Utah State University, Utah, United States
[‡]Department of Zoology, University of Otago, Dunedin, New Zealand

*Corresponding Author
E-mail: kim.hageman@usu.edu;
Telephone: 1-435-797-0114

For Submission to *Chemosphere*

ABSTRACT

A field study was conducted to further our understanding about the fate and transport of the organophosphate insecticide, chlorpyrifos, and its degradation product, chlorpyrifos oxon. Leaf, soil and air sampling was conducted for 21 days after chlorpyrifos application to a field of purple tansy (*Phacelia tanacetifolia*). Air samples were collected using a high-volume air sampler (HVAS) and seven battery-operated medium-volume active air samplers placed around the field and on a 0.5-km transect extending away from the field. Chlorpyrifos was detected every day of the sampling period in all matrices, with concentrations decreasing rapidly after application. Chlorpyrifos oxon was only detected in air samples collected with the HVAS during the first three days after application. Wind direction played a significant role in controlling the measured air concentrations in near-field samples. The SCREEN3 model and chlorpyrifos' Characteristic Travel Distance (CTD) were used to predict modeled chlorpyrifos concentrations in air along the transect. The concentration trend predicted by the SCREEN3 model was similar to that of measured concentrations whereas CTD-modelled concentrations decreased at a significantly

slower rate, indicating that downwind chlorpyrifos concentrations in air were primarily controlled by air dispersion. The SCREEN3-predicted chlorpyrifos concentrations were ~5 times higher than measured concentrations, indicating that simple approaches for calculating accurate pesticide fluxes are still needed. Finally, we found that measured concentrations in air on Days 0-2 at locations up to 0.5-km from the field were at levels considered concerning for human health.

1. INTRODUCTION

Pesticides applied to agricultural fields are subject to a number of fate processes including degradation, volatilization followed by off-site vapor drift, accumulation in soil or plants, and transport to surface or groundwater (Sarmah *et al.* 2004, Gao *et al.* 2012). Some of these processes lead to pesticide exposure for non-target organisms, including humans, and therefore pesticide concentrations are monitored and regulated in soil and water in most parts of the world, and in air but to a lesser extent (Li and Jennings 2017). The relative contribution of each process to pesticide fate depends on the physicochemical properties of the pesticide and other components of the formulation, properties of the soil and crop, and meteorological conditions (temperature, wind speed, relative humidity, and light intensity). The rates at which these processes occur are needed to determine how long pesticides are effective against pests and potentially harmful to humans and beneficial non-target organisms.

The environmental fate of pesticides has been the focus of many studies (e.g. Gao *et al.* 2012 and references). Herein, we focus on the semi-volatile organophosphate insecticide, chlorpyrifos (*O*,*O*-diethyl *O*-3,5,6-trichloropyridin-2-yl phosphorothioate, CAS No. 5598-15-2). Chlorpyrifos is one of the most frequently used insecticides in the world (Testai *et al.* 2010) but requires careful management due to a variety of demonstrated effects on non-target organisms

(John and Shaike 2015), including pollinators (Sanchez-Bayo and Goka 2014). Multiple studies have also shown that human prenatal exposure to chlorpyrifos can result in the development of autism, low birth-weight, attention deficit problems, and other developmental disorders (Perera *et al.* 2005, Rauh *et al.* 2011, Silver *et al.* 2017). Chlorpyrifos breaks down in the environment to chlorpyrifos oxon, which can be 10-1000 times more toxic than chlorpyrifos itself and can cause acute cholinergic neurotoxicity in organisms (Flaskos 2012, Armstrong *et al.* 2013). Due to these concerns, current chlorpyrifos regulations face increasing scrutiny (Mie *et al.* 2017, Centner 2018) and it has been banned in the US state of California (California Environmental Protection Agency 2019) and several countries (Pesticide Action Network International 2019).

Several studies have investigated chlorpyrifos behavior in agricultural fields after application. For example, Ngan *et al.* 2005 reported chlorpyrifos loss rates from soil following application. Antonious *et al.* 2017 reported chlorpyrifos and chlorpyrifos oxon loss rates from collard and kale foliage following application. Leistra *et al.* 2006 used micrometeorological methods to calculate chlorpyrifos volatilization rates from a potato field. Zivan *et al.* 2016 used measured concentrations at 70 m from a persimmon orchard and the pollutant dispersion model, CALPUFF, to estimate concentrations in air surrounding the orchard; however, their work led them to conclude that there is 'an urgent need for more measurements and modeling of atmospheric transport of pesticides to rural communities' and that 'estimations of post-application rates are still limited'. We also note that chlorpyrifos loss rates in soil, plants, and air have not been simultaneously measured in any of the previously mentioned studies so a comparison of loss rates from various media under identical conditions has not yet been possible. In addition, most studies have monitored chlorpyrifos concentrations post-application for 3-7 days and therefore more information is needed about its longer-term fate in an agricultural field.

The objective of this study was to advance understanding about chlorpyrifos behavior in agricultural environments by conducting a comprehensive investigation into its fate and loss rates post-application. Chlorpyrifos was applied to a field of purple tansy (*Phacelia tanacetifolia*) as part of a larger study on its effects on honey bees. Following its application, we measured chlorpyrifos and chlorpyrifos oxon concentrations in soil, leaves, and air for 21 days. Air samples were collected throughout the study period at seven locations around the field and along a transect extending 500 m from the field. To investigate the relative importance of dispersion versus depositional processes in controlling chlorpyrifos concentrations in air downwind of the field, we compared the measured concentrations of chlorpyrifos in air along the transect to those predicted using an air dispersion screening model, SCREEN3 (Lakes Environmental 2019, U.S. Environmental Protection Agency 2019) and using chlorpyrifos' Characteristic Travel Distance (CTD) (Bennett *et al.* 1998, Beyer and Matthies 2002). These two models were selected for comparison because SCREEN3 predicts dispersion for any non-reacting chemical or atmospheric particle whereas the CTD incorporates the physicochemical properties that affect a semi-volatile chemical's atmospheric fate. We also evaluated various methods for predicting chlorpyrifos volatilization flux, which is a key input parameter in SCREEN3, and compared measured concentrations in air to human health standards.

2. METHODS

2.1 Sampling Site, Pesticide Application, and Sampling Approach.

The experimental field (Figure 1 and Supplemental Information (SI) Figure S1) was located on a privately-owned farm in the Ida Valley, Central Otago, New Zealand (45°12´59.46´´ S; 169°42´6.56´´ E). The total area of the field was 1.26 ha and it was mostly surrounded by rocks

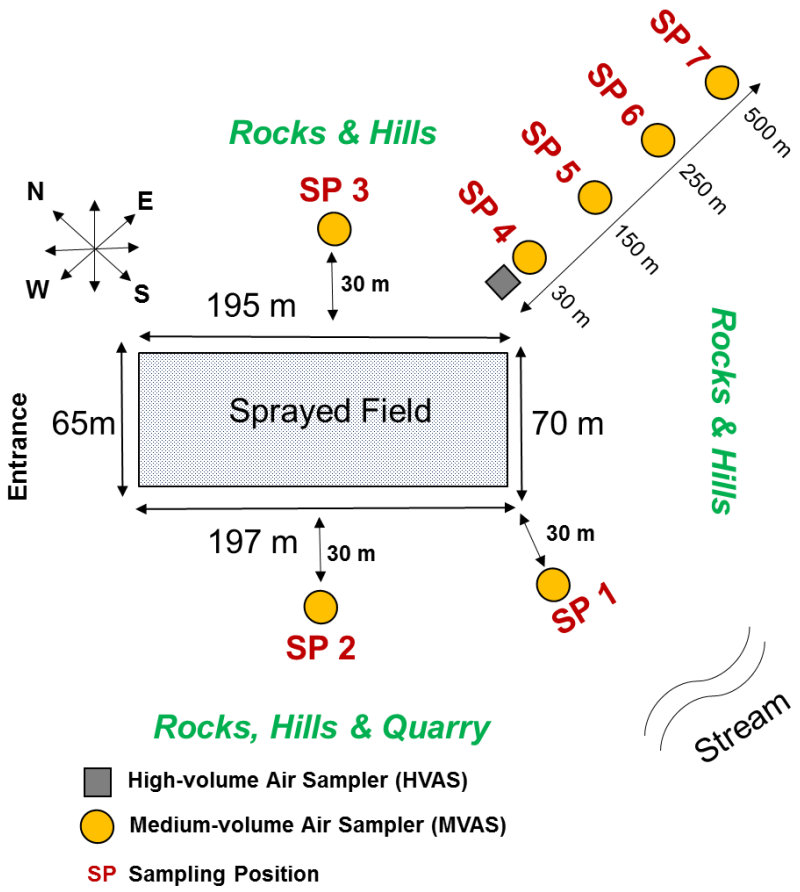

Figure 1. Experimental design indicating relative positions of sampling sites. In-field soil and leaf samples were collected at random locations within the sprayed field.

and small hills on three sides. Purple tansy (*Phacelia tanacetifolia*) seeds were sown on 21 October 2016. The field, with flowers in bloom, was sprayed with Lorsban™ 50EC (active ingredient: chlorpyrifos) on 8 January 2017 (austral summer) starting at 8 am. The spray application was carried out by a registered agrichemical contractor with a New Zealand Growsafe approved Agrichemical Handler Certification. On the morning of the application, the tank mixture was prepared according to label instructions (400 mL of Lorsban™ 50EC was added to 150 L of water) and the mixture was applied to the field using a 24-m spray boom mounted on a truck. Meteorological data were obtained from the nearest National Institute of Water and Atmospheric

Research (NIWA) station (Lauder, $45^0$2´24.36´´ S; 169^0 41´3.084´´ E). The air temperature was 10° C and the wind speed was 0 km hr^{-1} at the time of application.

Leaf and soil samples were collected from within the field. Air samples were collected at several sampling positions (SPs) located 30 m outside of the field and along a transect extending 500 m east of the field. After pesticide application, samples were collected for 21 days, using the schedule shown in Table S1. A high-volume air sampler (HVAS) and seven battery-operated medium-volume air samplers (MVASs) were used. The HVAS was used for three purposes: (a) its relatively high sampling rate (~220 L min^{-1}) ensured that even low concentrations of chlorpyrifos and its oxon would be detected, (b) it was used to calibrate the MVAS flow rate and (c) it could be used to separately sample particle-bound and gas-phase chemicals. The MVAS sampling rates were lower (28 L min^{-1}) and could not separate particle-bound and gas-phase chemicals, but did not require a power source so could be deployed at multiple locations around the experimental field and along the transect.

2.2 Leaf and Soil Sampling.

Leaf and soil samples were collected on each of the sampling days shown in Table S1. Purple tansy leaves (~8 g) were collected using gloved hands from randomly selected locations within the sprayed field. Surface soil samples (~10 cm deep), which were collected from the same in-field locations as leaves, were collected with a solvent-rinsed stainless steel sediment coring device. Leaf samples were stored in baked aluminum foil packets inside plastic zip-lock bags and soil samples were stored in pre-baked (400 °C) amber glass jars. All samples were stored at -20 °C and analyzed within ~120 days of sample collection.

Soil pH, measured using a standard method (Rayment and Lyons 2011) was 6.48 and 6.93 in two representative samples collected on a dry day (Day 2) and a wet day (Day 8), respectively. Total organic carbon, measured via the complete and instantaneous oxidation of the soil sample by flash combustion using a Flash Smart Elemental Analyzer (Thermo Scientific, MA, USA), was 3.0% and 2.2% in the two samples, respectively.

2.3 High-Volume Air Sampling.

A high-volume air sampler (HVAS) (PUF 3300BRL/230, Hi-Q Environmental Products Company, San Diego, CA) was deployed at SP 4, located 30 m from the eastern corner of the experimental field (Figure 1 and Figure S2). The HVAS was operated with a diesel generator because there was no power at the site. The sample cartridge head contained a 100-mm diameter quartz fiber filter (QFF) (Munktell, New Zealand) to collect particle-bound chemicals and a glass cartridge containing a polyurethane foam (PUF)/XAD-2 'sandwich' to collect gas-phase chemicals. The PUF/XAD-2 sandwich contained ~10 g XAD-2 resin (Restek, Australia) held between a 3-inch (6-cm diameter, 7.6-cm length) and 1-inch (6-cm diameter, 2.5-cm length) PUF plug (Restek, Australia). The HVAS was calibrated using a 10-cm adaptor plate (HI-Q Environmental Products Company, CA, USA) and a digital manometer (Testo 511, Testo AG, VIC, Australia). The mean flow rate was 220 L min^{-1}. Prior to use, all QFF and glass cartridges were baked for 4 h at 400 °C. PUF plugs and XAD-2 were cleaned prior to deployment using pressurized liquid extraction according to the method described in Section I of the SI and Table S2.

At ~8 am on each of the sampling dates shown in Table S1, a QFF and PUF/XAD-2 cartridge were installed in the HVAS. Following six hours of sampling, the sample cartridge and the QFF

were removed, wrapped separately with pre-baked aluminum foil, and stored in a zip-lock bag in an insulated container with ice blocks. After transporting samples to the laboratory, PUF and XAD-2 were separated from the cartridge and stored separately in amber glass jars at -20 °C until analysis (within ~120 days of sample collection). The 3- and 1-inch PUF plugs from the first three sampling events were stored and extracted separately for breakthrough analysis. The 3- and 1-inch PUF plugs from all other sampling events were stored and extracted together.

2.4 Medium-Volume Air Sampling.

The MVASs (SI Figure S3) were designed and built at the Department of Chemistry Workshop, University of Otago. Each sampler body was made of stainless steel. The two chambers inside the sampler were separated by a stainless steel plate with a 55-mm diameter hole in it. The bottom chamber contained a 12-V fan (ebm-papst Inc., Australia) while the upper chamber held the glass sampling cartridge. A glass sampling cartridge, containing a PUF/XAD-2 sandwich, was positioned between the lower plate and a removable cover, with rubber seals on both ends. The glass cartridges were identical to those used in the HVAS. A wind/rain shield was used to protect the sampling cartridge without blocking air flow. A digital timer was used to control the sampling time. Particles were not collected separately since the addition of QFF would have significantly decreased the flow rate; therefore, both particle-bound and gas-phase chemicals were trapped in the PUF/XAD-2 sampling cartridges.

MVASs were deployed at SPs 1-4 (Figure 1), which were located 30 m from the south corner, the southwest border, the northeast border and the east corner of the experimental field, respectively. Samples were not collected on the northwest border of the field due to the position of the field entrance. An additional three MVASs were deployed at SPs 5-7 (Figure 1) and formed

a transect extending 500 m to the east of the experimental field. The transect extended eastward because we expected it to be the dominant downwind direction. The 3- and 1-inch PUF plugs from the first three sampling events were stored and extracted separately for breakthrough analysis. At ~8 am on each of the sampling days, a PUF/XAD-2 cartridge was installed in the MVAS. After sampling for six hours, the sample cartridge was removed and stored in the same way as those used with the HVAS.

The flow rate of the MVAS located at SP 4 was calculated for each sampling date using the mass of chlorpyrifos measured in the MVAS cartridge ($M_{\text{CHL, MVAS}}$) and the chlorpyrifos concentration in air determined from the co-located HVAS ($C_{\text{CHL,air}}$) using equation 1. The volume of air sampled by the MVAS ($V_{\text{air,MVAS}}$) was calculated with equation 1,

$$V_{\text{air, MVAS}} = M_{\text{CHL, MVAS}} \times \frac{1}{C_{\text{CHL,air}}} \qquad \text{(Eq. 1)}$$

The mean MVAS flow rate, which was calculated by dividing $V_{\text{air,MVAS}}$ by the sampling time (6 h) for each of the nine sampling dates, was 28 L min^{-1}.

2.5 Chemicals.

High-purity dichloromethane (>99.98%), ethyl acetate (>99.9%), hexane (>98%), and acetone (>99.98%) were obtained from Merck (Germany). Chlorpyrifos was purchased from Fluka (Germany) and chlorpyrifos oxon from Thermo Fisher Scientific (MA, USA). Chlorpyrifos-d10 was obtained from Cambridge Isotope Laboratories (MA, USA).

199 **2.6 Analyte Extraction and Analysis.**

200 Chlorpyrifos and chlorpyrifos oxon were extracted from leaf, soil, and air sampling media
201 using pressurized liquid extraction with an Accelerated Solvent Extractor (ASE-350) from Thermo
202 Fisher Scientific (MA, USA). Chlorpyrifos was quantified with an Agilent 6890N gas
203 chromatograph coupled to an Agilent 5957 mass selective detector (GC-MS) (CA, USA).
204 Chlorpyrifos oxon was quantified with a Thermo Fisher Scientific TSQ Quantum Access MAX
205 Triple Quadruple Mass spectrometer (MA, USA). Detailed descriptions of the extraction and
206 instrumental procedures are provided in SI Sections II and III.

207 We did not target other potential chlorpyrifos degradation products, such as 3,5,6-trichloro-
208 2-methoxypyridinol and 3,5,6-trichloro-2-methoxypyridine, since previous studies have shown
209 that transformation to them is low relative to chlorpyrifos oxon (U.S. Environmental Protection
210 Agency 2018) and since they are not considered residues of concern due to relatively low toxicity
211 (U.S. Environmental Protection Agency 2011, Solomon *et al.* 2014).

212

213 **2.7 Quality Assurance.**

214 We quantified analytes in background samples, field blanks, and laboratory blanks. Method
215 recovery experiments for each sample matrix were conducted (Figure S4) and air sampling
216 methods were tested for breakthrough. Details regarding quality assurance can be found in SI
217 Section IV.

218

219 **2.8 Modelling Atmospheric Pesticide Transport.**

220 SCREEN3 is the screening version of the Gaussian plume Industrial Source Complex (ISC3)
221 model used by the US Environmental Protection Agency (EPA) (Lakes Environmental 2019, U.S.

Environmental Protection Agency 2019). It is designed to estimate maximum pollutant concentrations at defined distances from the pollutant source when the emission flux at the source is known. All SCREEN3 input parameters are provided in SI Table S5. In all simulations, we used the 'Area' option, a stability factor of 4 (default value), a wind speed of 5.9 m s^{-1} (the mean value during our first sampling period, Table S5), and the angle describing the transect extending to the east of our field (Figure 1). For the emission flux used in SCREEN3, we calculated a chlorpyrifos volatilization flux from the field using our measured leaf concentration, as described in SI Section V. We also tested several chlorpyrifos volatilization fluxes reported in the literature (Table S6), and one calculated using the approach of Woodrow *et al.* 1997 for comparison.

The CTD approach was developed to predict the transport potential of semi-volatile compounds in the atmosphere (Bennett *et al.* 1998, Beyer and Matthies 2002). CTD is the distance from the source region at which the concentration of a chemical is reduced by 63%. The ELPOS model uses the chemical and physical properties of the chemical to predict CTD. The ELPOS input parameters that we used are provided in Table S7. Equation 2 was used to generate ELPOS-modeled chlorpyrifos concentrations in air at distances downwind from the field (Bennett *et al.* 1998).

$$C_x = C_0 \, e^{(-x/CTD)} \qquad \text{(Eq. 2)}$$

where C_x is the concentration of pesticide in the air at distance x and C_0 is the concentration at the source, which is the agricultural field in our case.

3. RESULTS & DISCUSSION

3.1 Weather Conditions.

The pesticide application day was sunny with no rainfall, and the mean temperature during the 6-h sampling event was 18 °C (Table S8). The highest (27 °C) and lowest (13 °C) mean 6-h sampling period temperatures occurred on Days 2 and 12, respectively. The winds during sampling were relatively calm on the first two days of the study (Figures S5 and S6). After that, the strongest winds generally came from the northwest, with exceptions on Days 5 and 9 when the strongest winds came from the west and southeast, respectively. Figure S6 shows that during the first week after application, winds were calm in the morning and strong at night, with the strongest winds mainly coming from the northwest.

3.2 In-field Chlorpyrifos Concentrations in Leaves.

The mean concentration of chlorpyrifos in the first leaf samples collected after application (Day 0) was 21.6 μg g^{-1} (Figure 2 and Table S9). The concentration then dropped rapidly such that on Day 1, it was ~20% of the first measured concentration after application. Following this initial rapid loss, the concentration remained relatively constant until the end of the study. The final concentration of chlorpyrifos in leaves was 1.1 μg g^{-1} or ~5% of the initial concentration after application. The concentration trend was best described by a power curve, with the time for dissipation to half of the initial concentration (DT_{50}) being 0.4 h (Table S10). Chlorpyrifos oxon was not detected in leaves.

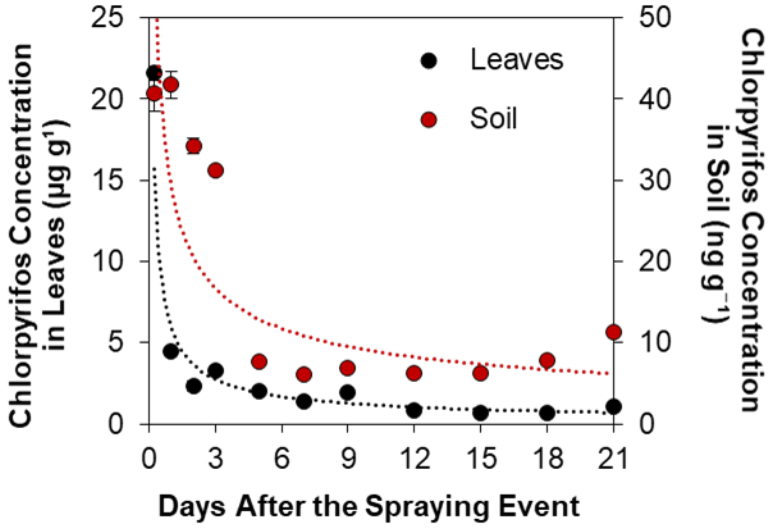

Figure 2. Chlorpyrifos concentrations in leaf and soil samples collected from within the field. Both fitted lines are power curves. Error bars, barely discernable in most cases, indicate ±1 standard deviation. All samples were analyzed in triplicate.

The range of DT_{50} values previously reported for chlorpyrifos dissipation from various leaf types is large (0.9 to 161 h) (Table S10). Interestingly, our DT_{50} value (0.4 h) was lower than any of these. Pesticide dissipation rates from leaves are affected by volatilization, wash-off with precipitation, and degradation. It did not rain during the first day of our study so wash-off was not responsible for the particularly fast loss rate. While it is possible that photodegradation occurred, the laboratory experiments conducted by Lester *et al.* 2017 showed that volatilization is the main pathway for chlorpyrifos loss from lemon leaves. Pesticide concentrations on leaf *surfaces* may decrease over time due to penetration into deeper layers; however, we measured the total concentration in leaves and not just that on the surface.

The variability in DT_{50} values observed in Table S10 may be due to a number of factors, including plant and field properties as well as meteorological conditions. Nonetheless, we note that the mean air temperature was similar during our experiment (18 °C) and that by Leistra *et al.* 2006 (21 °C), but the mean wind speed during our experiment (5.9 m s^{-1}) was much higher than

278 the range reported by Leistra *et al.* 2006 (2.3 to 3.5 m s^{-1}). Thus, wind speed likely contributed
279 significantly to the fast dissipation rate in our study. In any case, it is clear that chlorpyrifos DT_{50}
280 values from leaves are highly variable and that this research area could benefit from a more
281 systematic investigation into the factors that affect it. It is also worth noting that in some
282 experiments that report chlorpyrifos DT_{50} values from leaves, concentrations represent those on
283 leaf surfaces while in others (such as ours), they represent total concentrations. Significant
284 differences in surface versus total pesticide loss rates can be expected.

285 The chlorpyrifos concentration in leaves on Day 21 of our study was >20 times higher than
286 the maximum residue limits (MRLs) for leafy vegetables, herbs and edible flowers, which ranges
287 from 0.01 – 0.05 μg g^{-1} (European Food Safety Authority 2015). Although purple tansy is not a
288 harvestable crop and pesticide fate varies by plant species, this suggests chlorpyrifos residues in
289 edible leafy plants may be higher than expected and should be monitored carefully.

290

291 **3.3 In-field Chlorpyrifos Concentrations in Soil.**

292 The mean concentration of chlorpyrifos in the first soil samples collected after application
293 (Day 0) was 41 ng g^{-1} (Figure 2 and Table S9), which is ~500 times lower than that measured in
294 leaves on Day 0. This indicates that leaves intercepted most of the chlorpyrifos during application.
295 The chlorpyrifos concentration decreased, but not as rapidly as it did from leaves, such that on Day
296 1, the concentration was ~80% of the first measured concentration. From Day 5 to the end of the
297 study, the concentration was relatively stable and the concentration on the final day of the study
298 was 11.3 ng g^{-1}, or ~30% of the initial concentration. The concentration trend was best described
299 by a power curve, with the DT_{50} being 2 h (Table S10). Chlorpyrifos oxon was not detected in soil.

In a review of the fate of chlorpyrifos in the environment, Mackay *et. al*. 2014 reported DT_{50} values for chlorpyrifos in soil ranging from 168 to 720 h (7 to 30 d) (Mackay *et al.* 2014). Thus, our values and those reported by Ngan *et al.* 2005 are orders of magnitude lower than those reported by Mackay *et al.* 2014 or those measured by Montemurro *et al.* 2002 in an orange grove (Table S10). While our experiment and that of Ngan *et al.* 2005 were conducted with freshly applied chlorpyrifos, the rates reported by Mackay *et al.* 2014 were likely determined for 'aged' chlorpyrifos that had bound more tightly to soils over time. The orange grove studied by Montemurro *et al.* 2002 may have also contained aged chlorpyrifos. There is evidence that chlorpyrifos degrades faster in alkaline than acidic soils (Racke 1993); however, since our soils were slightly acidic, this does not explain the relatively fast loss we observed.

The chlorpyrifos concentrations we measured in soil were ~5 times lower than the median lethal dose for earth worms (210 ng g^{-1}) (Tomlin 2006), suggesting that ground-dwelling organisms may be largely protected from high pesticide exposure when plants intercept a high percentage of applied pesticides.

3.4 Near-field Chlorpyrifos and Chlorpyrifos Oxon Concentrations in Air.

The gas-phase chlorpyrifos concentrations reported in Figure 3 represent the total concentration found in PUF and XAD-2 using the HVAS; however, very little chlorpyrifos was found in XAD-2 (on average, the mass found in XAD-2 was 1.8% of that found in PUF; Table S11). On most sampling days, the gas-phase concentrations were also much higher than the particle-bound concentrations (Figure 3 and Table S11), which may simply be due to a low concentration of particles in air at our site.

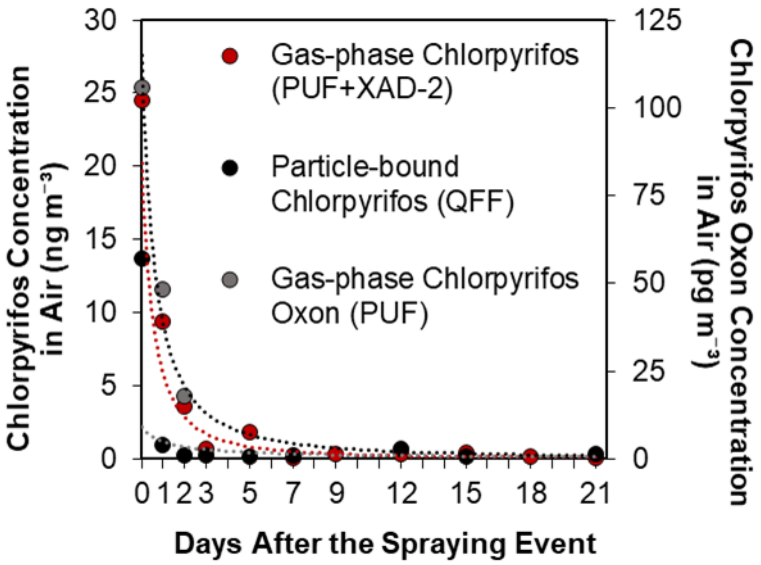

Figure 3. Gas-phase chlorpyrifos, gas-phase chlorpyrifos oxon, and particle-bound chlorpyrifos concentrations measured with HVAS at sampling position 4. All three fitted lines are power curves. Error bars are not shown since air sampling was not conducted in triplicate.

323 The gas-phase and particle-bound concentrations at SP 4 in the first samples collected after
324 chlorpyrifos application (Day 0) were ~24 ng m^{-3} and ~13 ng m^{-3}, respectively (Figure 3 and
325 Table S11). The concentrations in air decreased rapidly over the course of the study (Figure 3).
326 Again, concentration trends were best described by power curves; the DT_{50} of the gas-phase and
327 particle-bound chlorpyrifos were 13 and 0.3 h, respectively (Table S10). The particle-bound
328 concentrations may have decreased more rapidly than the gas-phase concentrations due to
329 particles generated during chlorpyrifos application quickly settling out. It is interesting that the
330 DT_{50} for gas-phase chlorpyrifos was much higher than it was for leaves or soil. Also, our DT_{50}
331 values for gas-phase chlorpyrifos were 3-4 times higher than those reported by Guardino *et al.*
332 1998 and Mackay *et al.* 2014. High variabilities in DT_{50} values for air from different studies are
333 not surprising since these values are highly dependent on meteorological conditions.

A deviation from the smooth decreasing concentration trend was observed on Day 5 when the gas-phase concentration was higher than expected. This increase was correlated with a switch in wind direction; on Days 0-4, winds mainly came from the northeast and northwest but on Day 5, they came from the west, i.e. directly across the sprayed field towards SP 4 (Figure S5 and Table S11).

The highest chlorpyrifos oxon concentration was 105.8 pg m^{-3} (Figure 3 and Table S11) and was measured in the first HVAS-PUF sample collected after application (Day 0). Chlorpyrifos oxon was detected in PUF but not in XAD-2. Zivan *et al.* 2016 also reported that chlorpyrifos oxon was not present in the XAD-2 used in their high-volume air sampler (Zivan *et al.* 2016). Our HVAS samples confirm the presence of chlorpyrifos oxon in air near the field until three days after the spray event (Figure 3 and Table S11). However, chlorpyrifos oxon concentrations were very low compared to chlorpyrifos concentrations. Interestingly, our DT_{50} for chlorpyrifos oxon was lower than that for chlorpyrifos (Table S10) whereas Mackay *et al.* 2014 reported the opposite relationship. Although chlorpyrifos oxon is more toxic than chlorpyrifos, our results support the conclusion drawn by Mackay *et. al.* 2014 that chlorpyrifos oxon concentrations in air near sprayed fields are not high enough to present a major concern.

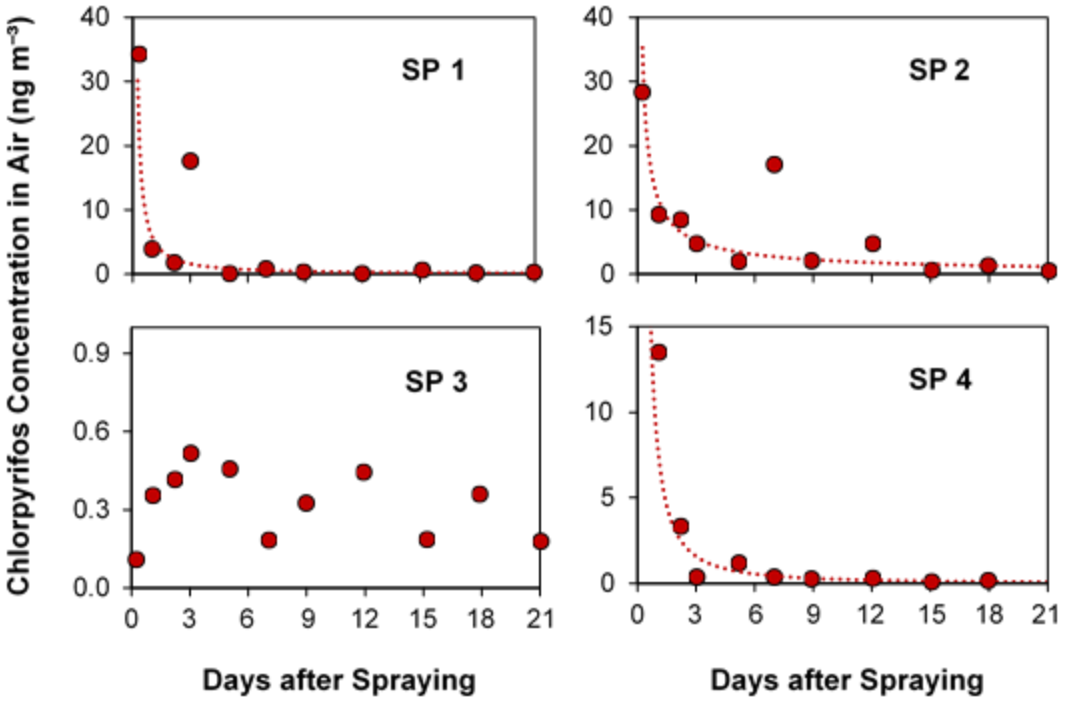

Figure 4. Chlorpyrifos concentrations measured with MVASs from sampling positions (SPs) 1-4. All three fitted lines are power curves. Error bars are not shown since air sampling was not conducted in triplicate.

The concentrations of chlorpyrifos at the various positions located at 30-m distances from the field, as determined by the MVASs, are shown in Figure 4. The highest concentrations were measured at SP 1 (34 ng m^{-3}) and SP 2 (28 ng m^{-3}) on Day 0 (Figure 4 and Table S12); these SPs were on the southern border of the field (Figure 1). This is not surprising since the strongest winds during the study came from the north (Figure S5). The concentrations in air decreased rapidly at all SPs except SP 3. Throughout the study, the concentrations at SP 3, which was on the northeast border of the field (Figure 1), were particularly low. This can be explained because no strong winds came from the southwest direction during the study. The deviations from expected concentrations observed at SP 1 on Day 3 and SP 4 on Day 5 can also be explained by shifts in wind direction on those respective days (Figure S5). Our results show that the pesticide concentrations in air during

the month following application can vary considerably on different sides of the sprayed field and that these variations can generally be explained by wind direction.

3.5 Chlorpyrifos Concentrations in Air along the Transect.

Figure S7 and Table S12 show the chlorpyrifos concentrations in air along the transect extending 500 m to the east of the sprayed field. Chlorpyrifos oxon was not detected in any of these samples, presumably because of the lower sampling rate of the MVAS compared to that of the HVAS. At SPs 4-6, the highest chlorpyrifos concentrations were measured in the first sample collected after application (Day 0) and rapid decreases were observed after that (Figure S7). It is interesting that this trend was not observed at SP 7, which was furthest from the experimental field. Although the SP 4 data on Day 0 is not available due to a sampling problem, it appears from the fitted curves that the concentration on Day 0 decreased along the transect from SP 4 to SP 7. An interesting spike in concentration was observed at SP 7 on Day 3. This spike may be explained because on the same day, the strongest winds were primarily blowing from the northwest (Figure S5), across the sprayed field towards the sampler transect.

3.6 Comparing Measured and Modeled Concentrations in Air along the Transect.

In the SCREEN3 model, the emission flux at the source strongly influences modelled chemical concentrations in air. For pesticide applications, the emission flux is equivalent to the volatilization flux from the field. In Table S6, we compared the chlorpyrifos volatilization flux calculated from our measured concentrations in leaves to previously reported rates determined using micrometeorological methods (Leistra *et al.* 2006, Mackay *et al.* 2014), as well as the flux estimated from vapor pressure using an empirical equation developed by Woodrow *et al.* 1997.

The reported chlorpyrifos volatilization rates cover several orders of magnitude and our calculated flux falls within this range. Since our approach is considerably simpler and cheaper than the ones reliant on micrometeorological measurements, and more field-specific than the estimation approach presented by Woodrow *et al*. 1997, it is worth further exploration as a viable alternative.

The SCREEN3-predicted chlorpyrifos concentrations obtained when using our calculated flux were ~5 times higher than the measured concentrations (Table S13). The predicted concentrations deviated further from measured values when using cited chlorpyrifos fluxes from the literature (Table S13), demonstrating that pesticide volatilization fluxes are not transferable between studies. The SCREEN3-predicted concentrations obtained when using the volatilization flux predicted using the empirical equation derived by Woodrow *et al*. 1997 (Table S6) were also much higher than our measured values (data not shown). Many factors related to the crop, field conditions, application protocol, and meteorology could affect the volatilization flux; most importantly, these results highlight the importance of volatilization flux on downwind concentrations and the need for accurate methods for predicting it.

To determine the effect of air dispersion on the chlorpyrifos concentrations we measured along the transect, we focused on the concentration *trend* produced by SCREEN3. This trend is affected by the air stability factor, but not by wind speed, field size, or the emission flux. To determine if the chlorpyrifos concentration trends we measured along our transect on Days 0, 1, and 2 were controlled primarily by air dispersion, we normalized the modelled concentrations so they matched those measured close to the field edge (Figure 5). These plots show that on all three days, the measured and SCREEN3-modelled concentration trends along the transect were very similar, indicating that the concentration trends were primarily controlled by air dispersion.

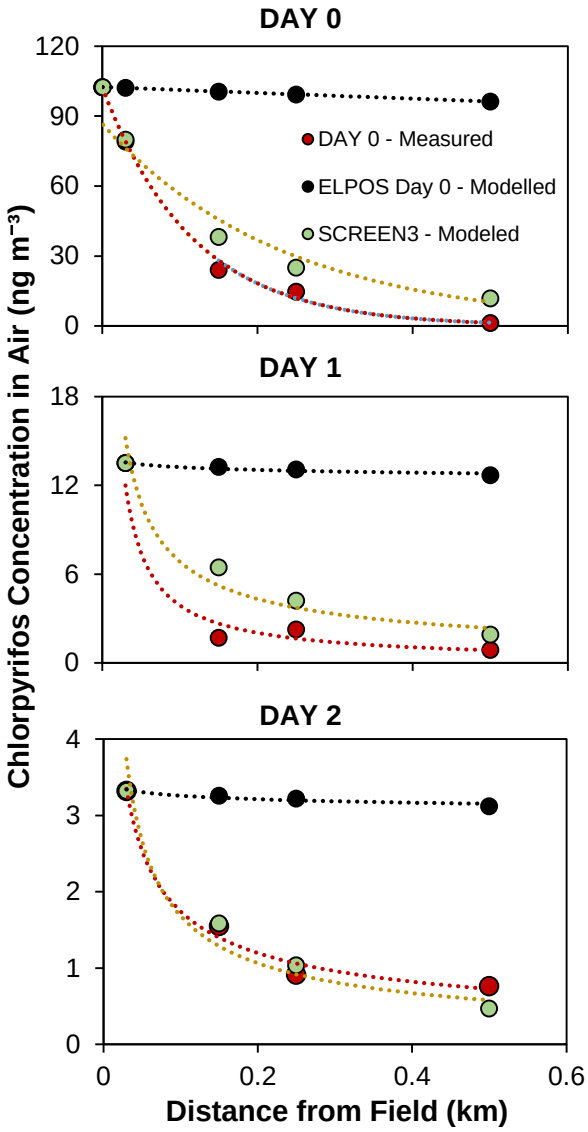

Figure 5. Measured, SCREEN3-modelled, and ELPOS-modelled chlorpyrifos concentrations on Days 0, 1, and 2 along the eastward-extending transect from our field site. Day 0 fitted lines are exponential while Day 1 and 2 fitted lines are power curves. Modeled concentrations were normalized to start at the same concentration as measured ones.

405 The CTD predicted by ELPOS (8 km) was used in Equation 2 to obtain the ELPOS-predicted
406 concentrations shown in Figure 5. Our initial measured concentrations were used as C_0 in Equation
407 2 so that the measured and modelled concentrations near the field edge were identical. The
408 concentration decrease predicted by the CTD was much lower than what we observed, indicating
409 that the change in chlorpyrifos concentration with distance from the field was not significantly

affected by deposition processes, which ELPOS is designed to predict. In sum, these results suggest that relatively simple air dispersion models like SCREEN3 should accurately predict concentration loss trends with distance from source for semi-volatile pesticides. However, SCREEN3 should be used with caution for pesticides that undergo more rapid degradation in the atmosphere and/or when meteorology is more complex that it was in study.

3.7 Comparison of chlorpyrifos concentrations in air to human health standards

A handful of human health standards for chlorpyrifos concentrations in air have been produced by US agencies; however, as indicated in the review by Li and Jennings 2017, such values are not available for other countries. The Texas short- and long-term hourly average Effects Screening Level concentrations for chlorpyrifos in air are 100 and 1000 ng m^{-3}, respectively (Texas Commission on Environmental Quality 2014). The US EPA uses reference concentrations ranging from 2.1 to 51 ng m^{-3} of chlorpyrifos in air in its Revised Human Health Risk Assessment for chlorpyrifos (U.S. Environmental Protection Agency 2016). The California EPA uses reference concentrations ranging from 4.1 to 8.6 ng m^{-3} chlorpyrifos its Final Toxic Air Contaminant Evaluation of Chlorpyrifos (California Environmental Protection Agency 2018). The reference concentrations quoted here are the Critical Points of Departure, which were calculated with a physiologically-based pharmacokinetic-pharmacodynamic (PBPK-PD) model (U.S. Environmental Protection Agency 2006), reduced by a factor of 100. Thus, the chlorpyrifos concentrations we measured in air on Days 0-2 up to 0.5 km from the field (Figure 5), and to some extent beyond Day 2 (Table S12) at various locations, were within the range of concern for human health according to the US and California EPA assessments. In their health assessments, the US EPA compared reference concentrations to those measured in several field experiments whereas

433 the California EPA compared reference concentrations to modelled concentrations generated with
434 the AGricultural DISPersal near-wake Lagrangian model (AGDISP) model using default
435 application scenarios. The use of measured and modelled data in these health assessments
436 highlights the importance of a thorough understanding of the factors that affect chlorpyrifos
437 concentrations in air in near- and downwind locations from sprayed fields.
438
439 **4. CONCLUSIONS**
440 Chlorpyrifos was detected in all in-field and near-field matrices (leaf, soil and air) at higher
441 than background concentrations until 21 days after application. Chlorpyrifos oxon was also
442 detected in near-field air samples with HVAS for the first three days after spraying. Chlorpyrifos
443 concentrations decreased rapidly in all matrices during the first several days after application.
444 Several observed concentration spikes could be explained by shifts in wind direction. The
445 concentrations measured on different sides of the field were remarkably varied and could generally
446 be explained by predominant wind directions. Measured chlorpyrifos trends generally agreed with
447 the SCREEN3 predicted trends. By contrast, ELPOS failed to predict those concentrations,
448 indicating that air dispersion was mainly responsible for the observed concentration trends along
449 the transect extending away from the field. The concentrations measured in air on Days 0-2, at
450 locations up to 0.5 km from the field, were at concentrations considered concerning for human
451 health.
452 Future research should focus on improving our understanding of the various field and
453 meteorological factors that affect pesticide DT_{50} values in leaves, soil, and air. This information
454 could be used to refine pesticide management decisions. For example, DT_{50} values on leaves and
455 soil control the length of time during which pesticides are effective against pests and harmful to

456 managed bees and beneficial insects. In addition, this research shows that better methods are
457 needed to predict and understand the emission rates of semi-volatile pesticides from agricultural
458 fields since reliable values are needed as input parameters in air dispersion models such as
459 SCREEN3. Among other things, air dispersion models can be used to predict pesticide inhalation
460 exposure to farmworkers and bystanders.
461
462 **5. ACKNOWLEDGEMENTS**

463 The authors especially wish to thank Garth Tyrrell and John Wells for their help with
464 designing and building the medium-volume active air samplers. For logistical and field assistance,
465 we would also like to thank the Paterson family (Ida Valley Station) and Tim Duncan (Duncan
466 Agricultural Contractors, Poolburn), Matthew Hayward (Department of Zoology, University of
467 Otago), and Robert Alumbaugh (Department of Pharmacology & Toxicology, University of
468 Otago). S. Das and S. Michelsen-Heath were sponsored by University of Otago PhD scholarships.
469
470 **6. SUPPLEMENTARY INFORMATION**

471 The supplementary information file contains additional details about methods,
472 meteorological conditions, and results, as well as tables of measured concentrations.
473
474 **7. REFERENCES**
475
476 Antonious, G. F., Turley, E. T., Abubakari, M. and Snyder, J. C. (2017). Dissipation, half-lives,
477 and mass spectrometric identification of chlorpyrifos and its two metabolites on field-grown
478 collard and kale. *Journal of Environmental Science and Health, Part B* **0**: 1-5.
479
480 Armstrong, J. L., Fenske, R. A., Yost, M. G., Galvin, K., Tchong-French, M. and Yu, J. (2013).
481 Presence of organophosphorus pesticide oxygen analogs in air samples. *Atmospheric Environment*
482 **66**: 145-150.
483

Bennett, D. H., McKone, T. E., Matthies, M. and Kastenberg, W. E. (1998). General Formulation of Characteristic Travel Distance for Semivolatile Organic Chemicals in a Multimedia Environment. *Environmental Science & Technology* **32**: 4023-4030.

Beyer, A. and Matthies, M. (2002). Criteria for atmospheric transport potential and persistence of pesticides and industrial chemicals. *German Environmental Agency, Report No. 02/2002*.

California Environmental Protection Agency. (2018). Final Toxic Air Contaminant Evaluation of Chlorpyrifos (https://www.cdpr.ca.gov/docs/whs/pdf/chlorpyrifos_final_tac.pdf) (Accessed October 2019).

California Environmental Protection Agency. (2019). California acts to prohibit chlorpyrifos pesticide (https://calepa.ca.gov/2019/05/08/california-acts-to-prohibit-chlorpyrifos-pesticide/) (Accessed June 2019).

Centner, T. J. (2018). Cancelling pesticide registrations and revoking tolerances: The case of chlorpyrifos. *Envrionmental Toxicology and Pharmacology* **57**: 53-61.

European Food Safety Authority (2015). Reasoned opinion on the refined risk assessment regarding certain maximum residue levels (MRLs) of concern for the active substance chlorpyrifos. *EFSA Journal* **13**: 4142.

Flaskos, J. (2012). The developmental neurotoxicity of organophosphorus insecticides: A direct role for the oxon metabolites. *Toxicology Letters* **209**: 86-93.

Gao, J., Wang, Y., Goa, B., Wu, L. and Chen, H. (2012). Environmental Fate and Transport of Pesticides. *Pesticides: Evaluation of Environmental Pollution*. H. S. Rathore and L. M. L. Nollet. Boca Raton, FL, CRC Press.

Guardino, X., Obiols, J., Rosell, M. G., Farran, A. and Serra, C. (1998). Determination of chlorpyrifos in air, leaves and soil from a greenhouse by gas-chromatography with nitrogen-phosphorus detection, high-performance liquid chromatography and capillary electrophoresis. *Journal of Chromatography A* **823**: 91-96.

John, E. M. and Shaike, J. M. (2015). Chlorpyrifos: pollution and remediation. *Environmental Chemistry Letters* **13**: 269-291.

Lakes Environmental. (2019). SCREEN View (https://www.weblakes.com/products/screen/index.html) (Accessed June 2019).

Leistra, M., Smelt, J. H., Hilbrand Weststrate, J., Van Den Berg, F. and Aalderink, R. (2006). Volatilization of the pesticides chlorpyrifos and fenpropimorph from a potato crop. *Environmental Science and Technology* **40**: 96-102.

Lester, Y., Sabach, S., Zivan, O. and Dubowski, Y. (2017). Key environmental processes affecting the fate of the insecticide chlorpyrifos applied to leaves. *Chemosphere* **171**: 74-80.

Li, Z. and Jennings, A. (2017). Worldwide regulations of standard values of pesticides for human health risk control: A review. *International Journal of Environmental Research and Public Health* **14**: 826.

Mackay, D., Giesy, J. P. and Solomon, K. R. (2014). Fate in the environment and long-range atmospheric transport of the organophosphorus insecticide, chlorpyrifos and its oxon. *Reviews of Environmental Contamination and Toxicology*. J. P. Giesy and K. R. Soloman. Heidelberg, Springer Open.

Mie, A., Rudén, C. and Grandjean, P. (2017). Safety of safety evaluation of pesticides: developmental neurotoxicity of chlorpyrifos and chlorpyrifos-methyl. *Environmental Health* **17**: 77.

Montemurro, N., Grieco, F., Lacertosa, G. and Visconti, A. (2002). Chlorpyrifos decline curves and residue levels from different commercial formulations applied to oranges. *Journal of Agricultural and Food Chemistry* **50**: 5975-5980.

Ngan, C. K., Cheah, U. B., Abdullah, W. Y. W., Lim, K. P. and Ismail, B. S. (2005). Fate of chlorothalonil, chlorpyrifos and profenofos in a vegetable farm in Cameron Highlands, Malaysia. *Water, Air, and Soil Pollution: Focus* **5**: 125-136.

Perera, F. P., Rauh, V., Whyatt, R. M., Tang, D., Tsai, W. Y., Bernert, J. T., Tu, Y. H., Andrews, H., Barr, D. B., Camann, D. E., Diaz, D., Dietrich, J., Reyes, A. and Kinney, P. L. (2005). A summary of recent findings on birth outcomes and developmental effects of prenatal ETS, PAH, and pesticide exposures. *Neurotoxicology* **26**: 573-587.

Pesticide Action Network International. (2019). Pan International Consolidated List of Banned Pesticides (http://pan-international.org/pan-international-consolidated-list-of-banned-pesticides/) (Accessed June 2019).

Racke, K. D. (1993). Environmental Fate of Chlorpyrifos. *Reviews of Environmental Contamination and Toxicology*. G. W. Ware. New York, Springer**:** 1-150.

Rauh, V., Arunajadai, S., Horton, M., Perera, F., Hoepner, L., Barr, D. B. and Whyatt, R. (2011). Seven-year neurodevelopmental scores and prenatal exposure to chlorpyrifos, a common agricultural pesticide. *Environmental Health Perspectives* **119**: 1196-1201.

Rayment, G. E. and Lyons, D. J. (2011). Soil Chemical Methods: Australasia (CSIRO Publications).

Sanchez-Bayo, F. and Goka, K. (2014). Pesticide residues and bees - a risk assessment. *Plos One* **9**: e94482.

Sarmah, A. K., Müller, K. and Ahmad, R. (2004). Fate and behaviour of pesticides in the acroecosystem - a review with a New Zealand perspective. *Australian Journal of Soil Research* **42**: 125-154.

578 Silver, M. K., Shao, J., Zhu, B., Chen, M., Xia, Y., Kaciroti, N., Lozoff, B. and Meeker, J. D.
579 (2017). Prenatal naled and chlorpyrifos exposure is associated with deficits in infant motor
580 function in a cohort of Chinese infants. *Environment International* **106**: 248-256.
581
582 Solomon, K. R., Williams, W. M., Mackay, D., Purdy, J., Giddings, J. M. and Giesy, J. P. (2014).
583 Properties and uses of chlorpyrifos in the United States. *Reviews of Environmental Contamination*
584 *and Toxicology*. **231:** 13-34.
585
586 Testai, E., Buratti, F. M. and Di Consiglio, E. (2010). Chapter 70 - Chlorpyrifos. *Hayes' Handbook*
587 *of Pesticide Toxicology (Third Edition)*. R. Krieger. New York, Academic Press**:** 1505-1526.
588
589 Texas Commission on Environmental Quality. (2014). Effects Screening Levels
590 (https://www.tceq.texas.gov/toxicology/esl/list_main.html) (Accessed October 2019).
591
592 Tomlin, C. D. S. (2006). The Pesticide Manual, A World Compendium, 14th Ed.; British Crop
593 Protection Council. Alton, UK.
594
595 U.S. Environmental Protection Agency (2006). Approaches for the Application of Physiologically
596 Based Pharmacokinetic (PBPK) Models and Supporting Data in Risk Assessment
597 (https://ofmpub.epa.gov/eims/eimscomm.getfile?p_download_id=458188) (Accessed October
598 2019).
599
600 U.S. Environmental Protection Agency. (2011). Revised chlorpyrifos preliminary registration
601 review drinking water assessment
602 (http://www.epa.gov/oppsrrd1/registration_review/chlorpyrfios/EPA-HQ-OPP-2008-0850-
603 DRAFT-0025%5B1%5D.pdf (Accessed September 2019).
604
605 U.S. Environmental Protection Agency. (2016). Chlorpyrifos: Revised Human Health Risk
606 Assessment for Registration Review (https://www.regulations.gov/document?D=EPA-HQ-OPP-
607 2015-0653-0454) (Accessed October 2019).
608
609 U.S. Environmental Protection Agency. (2018). Environmental transport and fate data analysis for
610 chlorpyrifos, Appendix 3-1. (https://www3.epa.gov/pesticides/nas/final/chlorpyrifos/appendix-3-
611 1.docx) (Accessed November 2018).
612
613 U.S. Environmental Protection Agency. (2019). Air Quality Dispersion Modeling - Screening
614 Models (https://www.epa.gov/scram/air-quality-dispersion-modeling-screening-models#screen3)
615 (Accessed June 2019).
616
617 Woodrow, J. E., Seiber, J. N. and Baker, L. W. (1997). Correlation techniques for estimating
618 pesticide volatilization flux and downwind concentrations. *Environmental Science and*
619 *Technology* **31**: 523-529.
620
621 Zivan, O., Segal-Rosenheimer, M. and Dubowski, Y. (2016). Airborne organophosphate pesticides
622 drift in Mediterranean climate: The importance of secondary drift. *Atmospheric Environment* **127**:
623 155-162.